



RSUIGM: Realistic Synthetic Underwater Image Generation with Image Formation Model

CHAITRA DESAI, KLE Technological University, Hubballi, INDIA

SUJAY BENUR, KLE Technological University, Hubballi, INDIA

UJWALA PATIL, KLE Technological University, Hubballi, INDIA

UMA MUDENAGUDI, KLE Technological University, Hubballi, INDIA

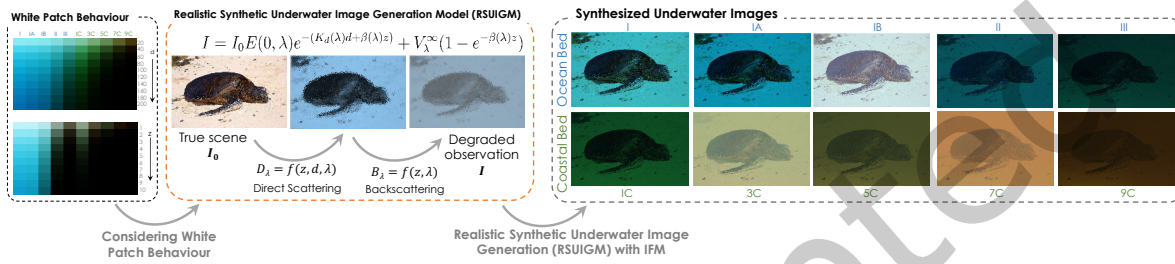


Fig. 1. Realistic Synthetic Underwater Image Generation with Image Formation Model. True scene (I_0) undergoes direct scattering and backscattering to form degraded observation (I). RSUIGM considers irradiance and radiance attenuation along downwelling depth d and line of sight distance z . We observe irradiance and radiance attenuation are interdependent, illustrated as white patch behaviour. We apply the proposed RSUIGM to generate synthetic underwater images for varying ocean beds and coastal beds.

In this paper, we propose to synthesize realistic underwater images with a novel image formation model, considering both downwelling depth and line of sight (LOS) distance as cue and call it as Realistic Synthetic Underwater Image Generation Model, RSUIGM. The light interaction in the ocean is a complex process and demands specific modeling of direct and backscattering phenomenon to capture the degradations. Most of the image formation models rely on complex radiative transfer models and in-situ measurements for synthesizing and restoration of underwater images. Typical image formation models consider only line of sight distance z and ignore downwelling depth d in the estimation of effect of direct light scattering. We derive the dependencies of downwelling irradiance in direct light estimation for generation of synthetic underwater images unlike state-of-the-art image formation models. We propose to incorporate the derived downwelling irradiance in estimation of direct light scattering for modeling the image formation process and generate realistic synthetic

Authors' addresses: Chaitra Desai, chaitra.desai@kletech.ac.in, Center of Excellence in Visual Intelligence (CEVI), School of Computer Science and Engineering, KLE Technological University, BVB Campus, Vidyanagar, Hubballi, Karnataka, INDIA; Sujay Benur, sujaybenur@gmail.com, Center of Excellence in Visual Intelligence (CEVI), School of Computer Science and Engineering, KLE Technological University, BVB Campus, Vidyanagar, Hubballi, Karnataka, INDIA; Ujwala Patil, ujwalapatil@kletech.ac.in, Center of Excellence in Visual Intelligence (CEVI), School of Computer Science and Engineering, KLE Technological University, BVB Campus, Vidyanagar, Hubballi, Karnataka, INDIA; Uma Mudenagudi, uma@kletech.ac.in, Center of Excellence in Visual Intelligence (CEVI), School of Computer Science and Engineering, KLE Technological University, BVB Campus, Vidyanagar, Hubballi, Karnataka, INDIA.

Permission to make digital or hard copies of all or part of this work for personal or classroom use is granted without fee provided that copies are not made or distributed for profit or commercial advantage and that copies bear this notice and the full citation on the first page. Copyrights for components of this work owned by others than the author(s) must be honored. Abstracting with credit is permitted. To copy otherwise, or republish, to post on servers or to redistribute to lists, requires prior specific permission and/or a fee. Request permissions from permissions@acm.org.

© 2024 Copyright held by the owner/author(s). Publication rights licensed to ACM.

ACM 1551-6857/2024/4-ART

<https://doi.org/10.1145/3656473>

underwater images with the proposed RSUIGM, and name it as *RSUIGM dataset*. We demonstrate the effectiveness of the proposed RSUIGM by using RSUIGM dataset in training deep learning based restoration methods. We compare the quality of restored images with state-of-the-art methods using benchmark real underwater image datasets and achieve improved results. In addition, we validate the distribution of realistic synthetic underwater images versus real underwater images both qualitatively and quantitatively. The proposed RSUIGM dataset is available here¹.

CCS Concepts: • Underwater image formation model; • Synthetic underwater images; • Restoration of underwater images;

1 INTRODUCTION

In this paper, we propose to generate realistic synthetic underwater images with a novel image formation model, referred to as Realistic Synthetic Underwater Image Generation Model (RSUIGM). The goal is to incorporate parameters affecting the appearance of underwater scenes, such as attenuation, scattering, and absorption of light, and simulate their effect of interactions with objects in the scene.

Modeling interaction of light with water is a complex phenomenon as properties of water are dynamic in nature. The presence of suspended particles, water temperature, salinity, and composition makes it challenging to model the behaviour of light. These factors cause scattering and absorption of light leading to degraded underwater images. Accurate estimation of optical properties in underwater scenario demands in-situ measurements. The in-situ measurements [29, 30] need complex equipments, skilled personnel, and are expensive. The cost of underwater imaging is expensive mainly due to the need for specialized equipment and expertise to overcome the challenges posed by the underwater environment, such as low visibility, turbulence, and limited illumination. Capturing of underwater images requires careful planning, execution, and deployment of specialized vehicles, such as ROVs (remotely operated vehicles) and AUVs (autonomous underwater vehicles) [27, 62]. The limited availability of underwater image datasets poses a major challenge for the development of deep learning models for underwater image analysis. Deep learning algorithms require large amounts of high-quality training data to achieve optimal performance, and the lack of such data has hindered the progress in this field.

In addition, underwater image analysis demands accurate ground-truth information to estimate various degradation parameters, such as color attenuation, backscatter, and turbidity. Ground-truth information provides a benchmark for comparing and validating the accuracy of the deep learning models. However, the underwater environment is often challenging for image acquisition due to aforementioned factors such as turbid water and poor lighting conditions, thus affecting the quality of the underwater images. Turbid water contains suspended particles, and leads to scattering of light, causing a reduction in contrast, color distortion, and blurring in images. Poor lighting conditions, results from absorption of light as it penetrates the water column, leading to a reduction in image brightness and color saturation. The challenges associated with capturing high-quality underwater images and the limited availability of datasets, coupled with the difficulty of acquiring accurate ground-truth information, makes the development of deep learning models complex and challenging task for underwater image analysis. To address these challenges, researchers [13, 28] propose to use synthetic data to train deep neural networks for underwater image analysis.

We observe that generation of synthetic underwater images is an overlooked problem and needs immediate attention. State-of-the-art methods focus on restoration of degraded observations without appreciating the need of ground-truth information for training deep neural networks. Towards this, we propose a novel image formation model, considering dependency of downwelling irradiance to generate synthetic underwater images. Generated synthetic underwater images and the corresponding ground-truth information paves ways for accurate estimation of degradation parameters, and facilitate improved restoration of degraded underwater images.

In particular, our contributions include:

¹<https://cevi.co.in/dataset/RSUIGM>, alternatively navigate through [https://cevi.co.in -> Datasets -> RSUIGM](https://cevi.co.in->Datasets->RSUIGM)

- We propose to synthesize realistic underwater images by considering both downwelling depth d and line of sight (LOS) distance z as cue in the image formation model. We call the proposed model as Realistic Synthetic Underwater Image Generation Model, RSUIGM.
 - We model the dependency of irradiance along d and z for estimation of direct light transmission. By doing so, we are able estimate direct light transmission in underwater environment effectively.
 - We analyse the variation in illumination across d and z using white patch behaviour towards validating RSUIGM.
- We propose a novel integral holistic approach, involving generation of synthetic underwater data, assessing the efficacy of synthetic data through restoration frameworks, and testing the restoration model with real underwater datasets. Towards this,
 - We generate a comprehensive dataset for training and testing of learning-based restoration framework, and call it as RSUIGM dataset.
 - We validate the distribution of synthetically generated data against real underwater images using Frechet Inception Distance (FID) quantitative metric and achieve enhanced scores on both UIEB and HICRD datasets.
 - We model one of the recent underwater image restoration frameworks, DepthCue [9] using RSUIGM dataset. We also model DepthCue using other benchmark *synthetic* underwater datasets such as RUIG [13] and SUID [28] to compare the quality of restored underwater images.
 - We extend the study to validate the characteristics of RSUIGM dataset by testing DepthCue architecture with benchmark *real* underwater datasets such as UIEB [39], UFO-120 [31], HICR [20] and EUVP [32] datasets. The results of restoration on real underwater images and synthetic underwater images proves the generated dataset encompasses the characteristics of real underwater datasets.
- We demonstrate the results of RSUIGM, with respect to synthetic data generation and restoration in comparison with SOTA methods using appropriate quality techniques.

In Section 2, we discuss about the relevant work carried out with respect to generation and restoration of degraded observations. In Section 3, we introduce the proposed realistic synthetic underwater image generation model (RSUIGM). In Section 4, we demonstrate the results with respect to synthetic underwater image generation considering restoration framework. In Section 5, we present conclusions on the proposed methodology.

2 RELATED WORK

In this section, we discuss recent works for generating synthetic underwater images considering restoration as a framework. We divide the literature in two phases: In first phase, we discuss literature on synthetic generation of underwater images and in second phase, we explore literature on restoration of underwater images.

2.1 Synthetic generation of underwater images

Researchers address the generation of synthetic underwater images in two ways namely a) Image Formation Model based methods and b) Learning-based methods. Approaches based on image formation models [15, 22, 51] consider traditional dehazing models [4, 16, 18, 19, 23, 60, 61] for restoration of degraded underwater images. However, these models are limited to atmospheric conditions and do not accurately reflect the behaviour of light in underwater scenario. Typically, the behaviour of light in water differs significantly from atmosphere and requires a corresponding image formation model for accurate generation of underwater images.

Authors in [28] use traditional image formation model proposed by [43] to synthetically generate underwater images. However, this model only considers the attenuation of light along the line of sight and ignores the effect of irradiance attenuation, resulting in color distortions. Authors in [54] consider the irradiance attenuation to synthesize the underwater images, however the image formation model proposed includes absorption and scattering

coefficients in modelling irradiance attenuation. Desai et al. [11–13] considers revised image formation model [1] to synthesize underwater images. The synthetic underwater images coupled with ground-truth information are used to train deep learning models for restoration. However, the image formation model considered [1] are sensitive to in-situ measurements for estimation of attenuation coefficients. In-situ measurements demands complex and expensive instrumentation and a skilled personnel to handle these complex equipments. Authors in [1] include beam attenuation coefficient β_λ in direct light estimation leading to inappropriate assumptions on irradiance pattern.

From literature, we infer estimation of attenuation of light along the water column across all wavelengths and water types facilitate to determine the true behaviour of light along the line of sight leading to improved color restoration. According to Jaffe et al. [34], the estimation of radiance reflected from an object requires the estimation of the irradiance pattern incident on the object surface. Solonenko et al. [49] introduced an explicit way to measure the downwelling irradiance $E(d, \lambda)$, from which we can estimate diffuse downwelling attenuation coefficient $K(d, \lambda)$. However, we observe synthetic underwater image generation and its usage towards restoration finds limitations as it is sensitive to both attenuation of light across the water column and line of sight. Towards this, we intuitively estimate a parameter for estimation of irradiance incident across the water column and line of sight.

The alternate way to synthesize underwater images include generative models. Authors in [41] and [55] use generative adversarial models to render realistic underwater images however, the underlying imaging model for rendering is an atmospheric dehazing model. The atmospheric dehazing model does not consider the effect of backscattering present in underwater environments, resulting in color cast and haze during image restoration. Synthesizing underwater images using generative models demand ground-truth images and the corresponding degraded observations to mimic the wide range of water types. However, training the discriminator network on such a diverse distribution of samples is practically infeasible. Towards this, we propose a Realistic Synthetic Underwater Image Generation Model (RSUIGM) for synthesizing underwater images considering dependency of ambient spectrum along d and z .

2.2 Restoration of underwater images

Unlike image enhancement [25, 26, 35, 36, 44], restoration is an objective process and tends to recover true scene from degraded observation using image formation model. However, the image formation process in underwater environment is sensitive to both Inherent Optical Properties (IOP's) and Apparent Optical Properties (AOP's) of the water. Through literature we infer, inherent optical properties are primarily responsible for the degradation of underwater scenes during the capture [49]. Recovering the lost colors and other information of underwater scene is feasible either through In-situ measurements of IOP's [29, 30] or deep learning approach [38, 40, 42, 60].

To overcome aforementioned challenges, we propose a novel method of generating underwater images by incorporating physical principles, such as the Beer-Lambert law [57], and scattering [6] theory for simulating the image formation process in underwater environment. The proposed model (RSUIGM) also considers the influence of factors such as downwelling depth and line of sight distance in synthesizing wide range underwater scenes. We develop an algorithm to generate underwater images without any in-situ measurements of the IOP's. We propose to train deep learning models using RSUIGM dataset for restoration of degraded underwater images.

3 REALISTIC SYNTHETIC UNDERWATER IMAGE GENERATION MODEL (RSUIGM)

In this section, we propose a novel image formation model for underwater scenario considering both downwelling depth and line of sight distance towards synthesizing underwater images. The proposed model (RSUIGM) estimates the parameters of the distribution describing the synthetic underwater images. Sampled realistically rendered underwater images are then generated from this learnt distribution. This approach allows the proposed

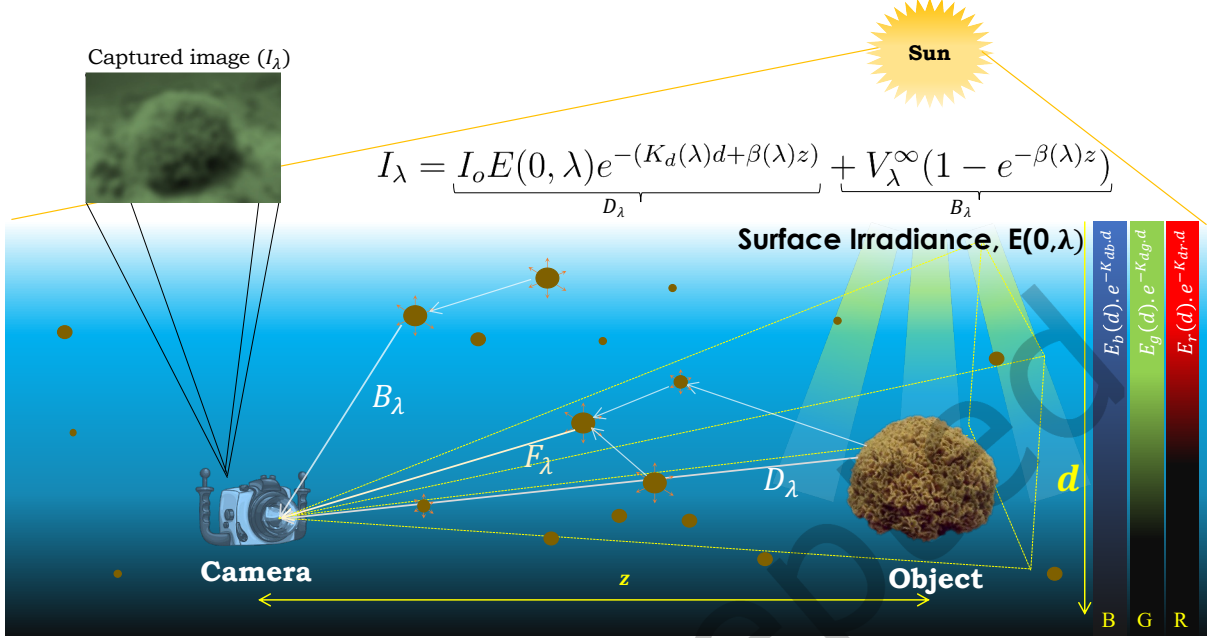


Fig. 2. Image formation in underwater scenario. Light reaching the camera undergoes Direct light attenuation (D_λ), Backscattering (B_λ) and Forward scattering (F_λ) resulting in degraded observation (I_λ). Quality of restoration is sensitive to light reaching the object $E(d, \lambda)$, and in-turn irradiance is sensitive to depth and wavelength. Ideally at $d = 0$, $E(0, \lambda)$ (i.e at the surface), we observe no color distortion. $E(d, \lambda)$ attenuation along d across R, G, B is shown in extreme right hand side of the figure.

model to generate a diverse set of realistically rendered underwater images, showcasing its ability to capture the complexities inherent in underwater environments. Typically in underwater scenario, the true scene (I_o) undergoes Direct scattering (D_λ), Backscattering (B_λ), and Forward scattering (F_λ) resulting in degraded observation (I_λ) as shown in Fig 2. Most of the authors in literature [18, 51, 58] model the image formation process considering attenuation along line of sight. However, the underwater image formation is sensitive to both (i) downwelling irradiance attenuation and, (ii) attenuation of light along line of sight. The downwelling irradiance $E(d, \lambda)$ is a function of depth d and wavelength λ . Downwelling depth d refers to the depth at which light penetrates the water column, and varies depending on the wavelength of light and the properties of the water. Line of sight distance z refers to the distance between the camera and the object being imaged, and affects the amount of light that reaches the camera. Ideally at $d = 0$, i.e. $E(0, \lambda)$ at the surface of water the distortions are assumed to be negligible and gradually increases with d . To address this, we incorporate downwelling depth and line of sight distance into the image formation model for accurate estimation of the optical properties underwater, resulting in clearer and natural-looking underwater images.

The irradiance along the water column attenuates with downwelling depth d and is directly proportional to radiance reaching the camera along LOS and is given by,

$$I(\lambda, d, z) \propto I_o(\lambda, d_0, z_0) \quad (1)$$

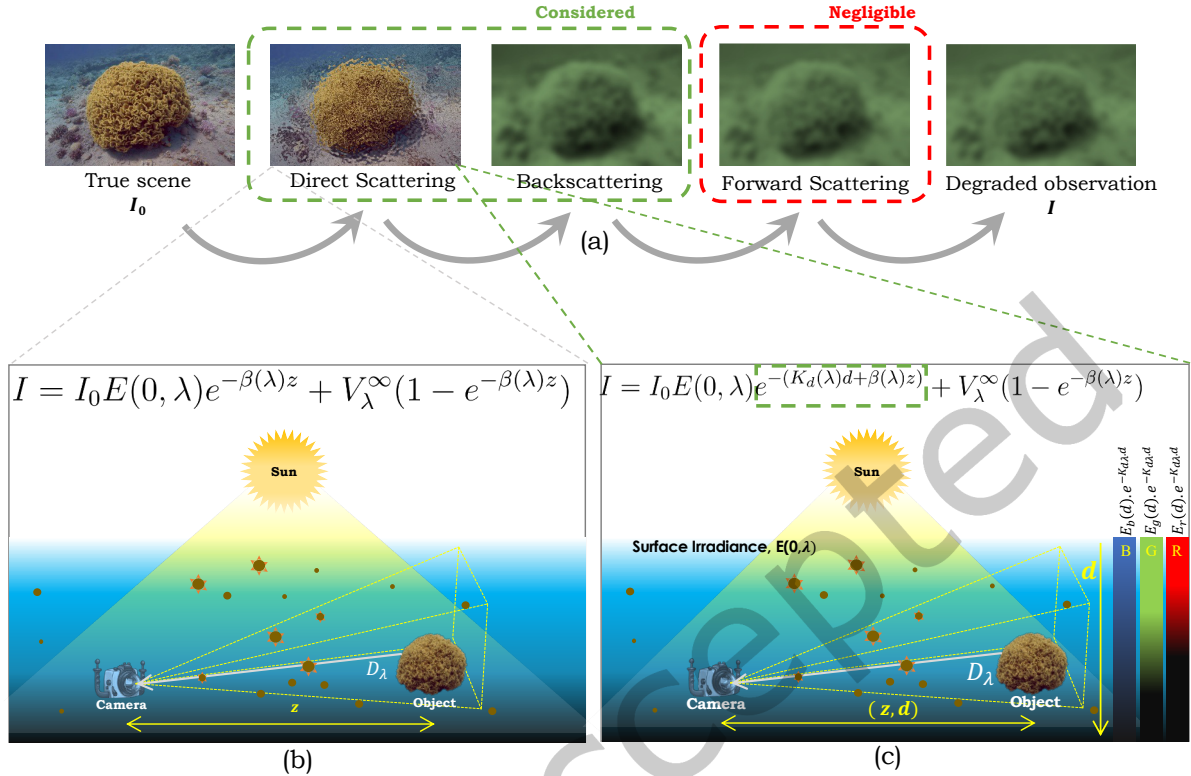


Fig. 3. Proposed image formation model based on the light rays reaching the observer from the object/scene under imaging. (a) True scene $I_0(\lambda, d_0, z_0)$ undergoes Direct Scattering, Backscattering and Forward Scattering resulting in degraded observation $I(\lambda, d, z)$. (b) Direct scattering modelled as a function of z . (c) Proposed image formation model, where Direct scattering is modelled as a function of both (d, z) .

where, $I(\lambda, d, z)$ is the captured image and $I_o(\lambda, d_0, z_0)$ is the true scene considering d_0 i.e at $d = 0$ and z_0 i.e at $z = 0$.

Conventionally, the propagation of light from the object to the camera in underwater scenes is governed by radiance transfer equation (RTE) [6]. RTE is sensitive to the variation in downwelling depth d and LOS distance z , across all wavelengths. The simplest form of RTE considering homogeneous water type (i.e ignoring the effects of Apparent Optical Properties (AOP's)) is given by,

$$I(\lambda, d, z) = \underbrace{I_o e^{-\beta(\lambda)z}}_{D_\lambda} + \underbrace{I_B(1 - e^{-\beta(\lambda)z})}_{B_\lambda} + I_F \quad (2)$$

Direct light attenuation D_λ in Equation 2, is the effect resulting from photons colliding with suspended particles, while traveling from the object to camera along LOS distance z . The Backscattering B_λ , in the Equation 2, is the additional radiance reaching the camera due to photons colliding with each other in all other directions excluding line of sight. Forward scattering I_F in Equation 2 is the effect resulting from reflection of light by the objects excluding the line of sight. However, due to collision the photons reorient along the line of sight. We ignore the

effect of forward scattering in image formation, as the effect of forward scattering is minimal [14, 47, 52]. Hence, the Equation 2 reduces to Equation 3 and is given by,

$$I_\lambda = D_\lambda + B_\lambda \quad (3)$$

However, the authors in [13, 18, 23, 28, 51, 58] consider attenuation along z in synthesizing underwater images, and do not explicitly model the effect of downwelling depth d . Modeling the effect of downwelling depth is crucial for generating realistic underwater images, as it significantly affects the appearance and color of objects in the scene. Ignoring the effect of d [34] leads to inaccurate modeling of direct light transmission in underwater image formation process introducing color distortions in underwater images.

In what follows, we model the Direct Scattering D_λ and Backscattering B_λ in Realistic Synthetic Underwater Image Generation Model (RSUIGM).

3.1 Direct Scattering (D_λ)

In this section, we propose a novel method for estimation of direct scattering (D_λ). We reiterate, direct light attenuation, is the effect resulting from photons colliding with suspended particles, while traveling from the object to camera along LOS distance z . Fig 3(a) shows, image formation process where true scene I_o undergoes direct scattering (D_λ), backscattering (B_λ), and forward scattering (F_λ) resulting in degraded observation (I_λ). Most of the authors [18, 51, 58] in literature consider attenuation of light only along the line of sight distance z for modeling the effect of Direct Scattering (D_λ) in the image formation process, and ignore the effect of downwelling irradiance along depth d shown in Fig 3(b). However as per [34] it is essential to estimate the downwelling irradiance pattern to determine the effect of D_λ along the line of sight distance z . Towards this, we propose to model the dependency of downwelling irradiance pattern along d and z for determining the effect of D_λ in image formation process.

Attenuation of light due to absorption and scattering in any medium as given by Beer-Lambert's law [57] as a function of,

$$I = f(I_o, a, s, z, \lambda) \quad (4)$$

where, a and s are absorption and scattering coefficients respectively. The Beer-Lambert's law can be represented as,

$$I_\lambda = I_o e^{-(a+s)*z} \quad (5)$$

Considering the theory of Beer-Lambert's law [57] most of the authors in literature model the effect of D_λ as,

$$D_\lambda = f(I_o, a, s, z, \lambda) \quad (6)$$

Image formation models proposed in literature [1, 4, 23, 46] ignore the dependency of downwelling irradiance across d for estimating the effect of direct light scattering. According to Jaffe et al. [33, 34], it is essential to estimate the downwelling irradiance pattern $E(d, \lambda)$ incident on the object to estimate the radiance reflected from an object. To accomplish this, Solonenko et al. [49] have presented an explicit method to measure the downwelling irradiance $E(d, \lambda)$, which can subsequently be used to estimate downwelling diffuse attenuation coefficient $K(d, \lambda)$. The quasi apparent optical property $K(d, \lambda)$ is an attenuation coefficient to measure penetration of light along the water column [56]. Through literature, we infer the performance of both generating synthetic underwater images and restoration of underwater images is limited as it is sensitive to attenuation of downwelling irradiance across d and z . We show d and z are interdependent through Fig 4 and remodel the Equation 6 accordingly,

$$D_\lambda = f(I_o, a, s, z, \lambda, d) \quad (7)$$

Substituting Equation 6 in Equation 3, we get

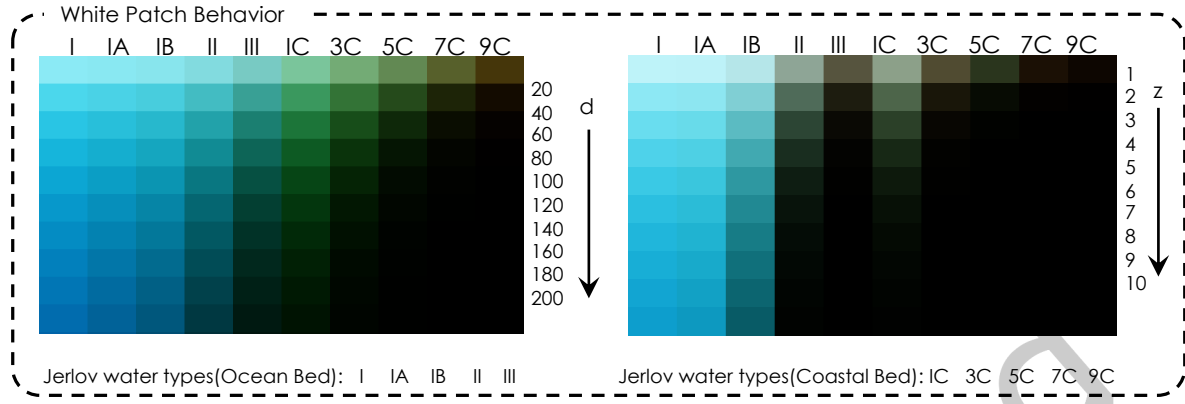


Fig. 4. White patch behaviour for varying downwelling depth (d in meters) considering $z = 0$ (left image), White patch behaviour for varying distance (z in meters) along LOS considering $d = 0$ (right side), White patch behaviour shows irradiance and radiance attenuation are sensitive to both the depth d and z respectively and are interdependent.

$$I_\lambda = I_o e^{-(a+s)*z} + B_\lambda \quad (8)$$

$$\implies D_\lambda = I_o e^{-(a+s)*z} \quad (9)$$

Equation 9, is necessary but not sufficient in estimation of direct light transmission, as it ignores the effect of irradiance attenuation along d . Towards this, we consider to introduce the effect of irradiance attenuation $E(d, \lambda)$ in Equation 9,

$$D_\lambda = I_o E(d, \lambda) e^{-(a+s)*z} \quad (10)$$

According to Jaffe et al. [34] the irradiance at depth d i.e $E(d, \lambda)$ is directly proportional to surface irradiance $E(0, \lambda)$ i.e,

$$E(d, \lambda) \propto E(0, \lambda) \quad (11)$$

$$E(d, \lambda) = T(d, \lambda) E(0, \lambda) \quad (12)$$

where, the proportionality constant $T(d, \lambda)$ is irradiance transmittance across d and λ . The irradiance transmittance is sensitive to diffused downwelling attenuation coefficient ($K_d(\lambda)$) and is given by,

$$T(d, \lambda) = e^{-K_d(\lambda)d} \quad (13)$$

Unlike SOTA methods [1, 3], we propose to combine the attenuation of light along d and z using principles of Beer-Lambert's law [57], Jaffe et al. [34] and Solonenko et al. [49] in estimation of direct light transmission (D_λ) as given in Equation 14,

$$D_\lambda = I_o E(d, \lambda) e^{-\beta(\lambda)z} \quad (14)$$

where, $E(d, \lambda)$ is ambient spectrum as depicted in Equation 12. $E(d, \lambda)$ considers the dependency of ambient spectrum on diffused downwelling attenuation coefficient ($K_d(\lambda)$). The Equation 14 further reduces to,

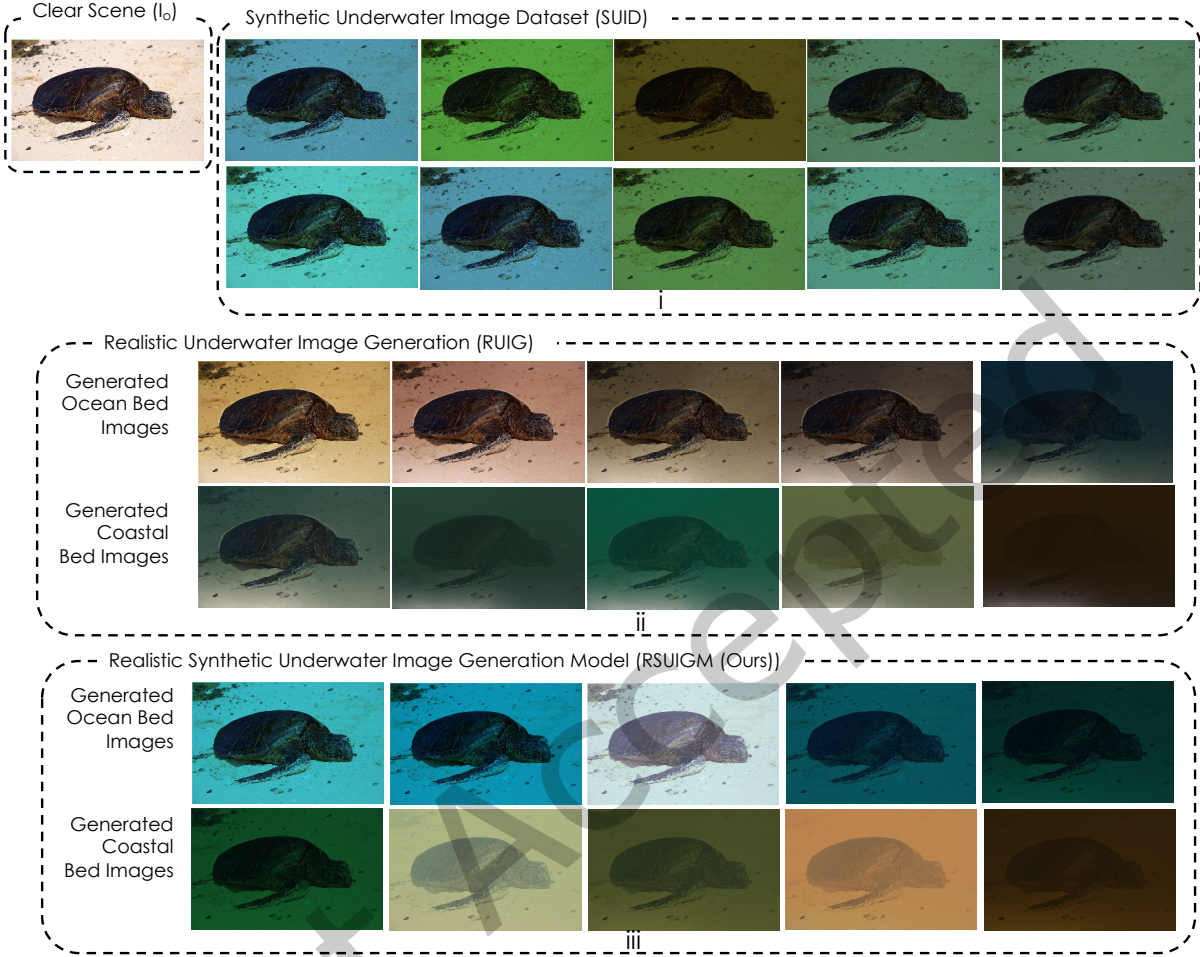


Fig. 5. Comparison of state-of-the-art image formation models for generation of synthetic underwater images i) Generation of synthetic underwater images by authors in [28], ii) Generation of synthetic underwater images by authors in [13], iii) Generation of synthetic underwater images with proposed RSUIGM (ours).

$$D_\lambda = I_o e^{-K_d(\lambda)d} E(0, \lambda) e^{-\beta(\lambda)z} \quad (15)$$

$E(0, \lambda)$, i.e., irradiance at the surface is ideally 1. The Equation 15 can be rewritten as (see Fig 3(c)),

$$D_\lambda = I_o e^{-(K_d(\lambda)d+\beta(\lambda)z)} \quad (16)$$

Backscattering (B_λ): The additional radiance gained in LOS leads to backscattering (B_λ) as shown in Equation 17. B_λ introduces haze in the underwater scene. We estimate B_λ using the technique discussed in [1] and is shown in Equation 17,

$$B_\lambda = V_\lambda^\infty (1 - e^{-\beta(\lambda)z}) \quad (17)$$

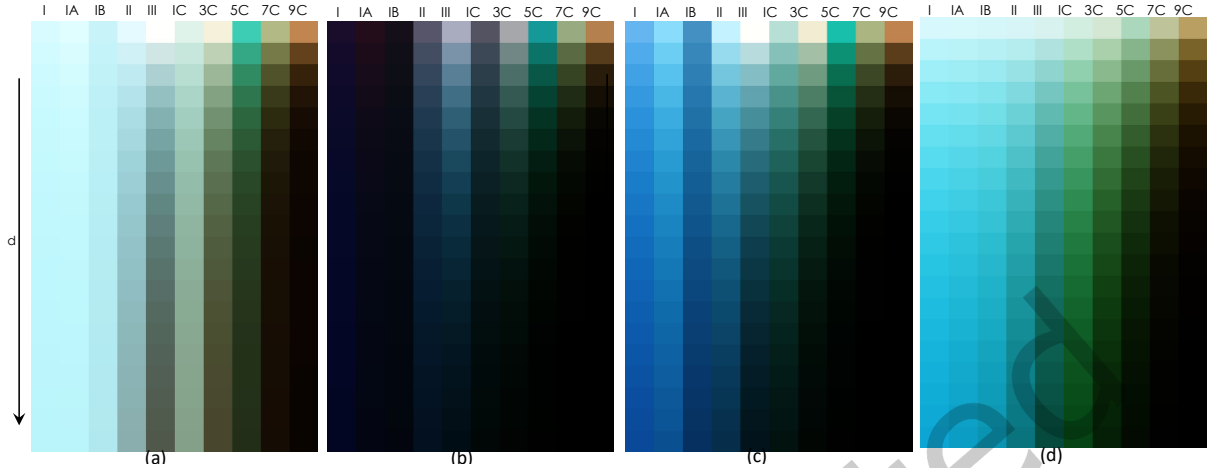


Fig. 6. White patch behaviour of $K_d(\lambda)$ and $\beta(\lambda)$ for both direct light scattering and backscattering degradations. (a) $I_\lambda = I_o E(0, \lambda) e^{-(\beta(\lambda)d + \beta(\lambda)z)} + V_\lambda^\infty (1 - e^{-\beta(\lambda)z})$, (b) $I_\lambda = I_o E(0, \lambda) e^{-(K_d(\lambda)d + K_d(\lambda)z)} + V_\lambda^\infty (1 - e^{-\beta(\lambda)z})$, (c) $I_\lambda = I_o E(0, \lambda) e^{-(K_d(\lambda)d + K_d(\lambda)z)} + V_\lambda^\infty (1 - e^{-K_d(\lambda)z})$, (d) $I_\lambda = I_o E(0, \lambda) e^{-(K_d(\lambda)d + \beta(\lambda)z)} + V_\lambda^\infty (1 - e^{-\beta(\lambda)z})$ (RSUIGM), White patch behaviour shows absorption and scattering phenomena are sensitive to both d and z .

B_λ is sensitive to V_λ^∞ (backscattering for object at infinity). V_λ^∞ is a function of scattering coefficient $s(\lambda)$, additive coefficient $\beta(\lambda)$ (summation of absorption and scattering coefficient) and $E(d, \lambda)$ as shown in Equation 18,

$$V_\lambda^\infty = \frac{s(\lambda)E(d, \lambda)}{\beta(\lambda)} \quad (18)$$

As discussed previously in Equation 3, the total radiance (I_λ) reaching the observer is,

$$I_\lambda = D_\lambda + B_\lambda$$

Substituting Equation 16 and Equation 17 in Equation 3 we get,

$$I_\lambda = I_o E(0, \lambda) e^{-(K_d(\lambda)d + \beta(\lambda)z)} + V_\lambda^\infty (1 - e^{-\beta(\lambda)z}) \quad (19)$$

Equation 19 shows, the total radiance reaching the observer from the object results in degraded image I_λ . Considering the parameter ($K_d(\lambda)$) in image formation process is essential for determining the amount of irradiance reaching the sensor from the object due to direct scattering effect. Traditional image formation models relaxed upon the assumption of d and ($K_d(\lambda)$) in determining amount of radiance reaching the sensor leading to inconsistencies in synthetic data generation processes. By considering this specific attenuation parameter into the modeling process, we are able to simulate interaction of irradiance with water constituents, facilitating generation of realistic synthetic data. This parameter is also necessary for reproducing tinting effect observed in underwater scenes. We observe, considering the attenuation of light along d and z in estimation of direct light transmission facilitates realistic synthetic generation of underwater images and ensures the quality of restoration.

3.2 Effect of $K_d(\lambda)$ and $\beta(\lambda)$

In this section, we discuss on the behaviour of $K_d(\lambda)$ and $\beta(\lambda)$ attenuation coefficients and show they are independent phenomenon. Both the attenuation coefficients contribute to the degradations introduced in the

image formation process underwater. Attenuation coefficient, $K_d(\lambda)$ determines the rate at which the downwelling irradiance, i.e., the irradiance of the light entering the water surface, is absorbed and scattered as it travels through the water column. Attenuation coefficient, $\beta(\lambda)$ models absorption and scattering phenomenon along line of sight distance z . The attenuation of light along d is typically higher for shorter wavelengths of light, such as blue and green, than for longer wavelengths, such as red and infrared leading to a reduction in the intensity of the downwelling irradiance with increasing depth. Towards this, we conduct experiments to determine the effects of $K_d(\lambda)$ and $\beta(\lambda)$ using different scenarios on the image formation process. Through experimentation, we observe different degradations in image formation process due to variations introduced in $K_d(\lambda)$ and $\beta(\lambda)$. We perform experiments under direct scattering, backscattering and combination of direct scattering and backscattering as 3 different scenarios to understand the individual effects of these parameters.

- Scenario 1 (Combining direct scattering and backscattering): Ignoring the effect of diffused downwelling irradiance attenuation $K_d(\lambda)$ in estimation of both direct and backscattering phenomenon.
i.e. $I_\lambda = I_o E(0, \lambda) e^{-(\beta(\lambda)d+\beta(\lambda)z)} + V_\lambda^\infty (1 - e^{-\beta(\lambda)z})$
- Scenario 2 (During direct light scattering): When $\beta(\lambda)$ is replaced by $K_d(\lambda)$ in direct light attenuation, i.e. $K_d(\lambda)$ influencing both absorption and scattering phenomena along the LOS distance z during direct light scattering.
i.e. $I_\lambda = I_o E(0, \lambda) e^{-(K_d(\lambda)d+K_d(\lambda)z)} + V_\lambda^\infty (1 - e^{-\beta(\lambda)z})$
- Scenario 3 (During backscattering): Considering the influence of direct light attenuation $K_d(\lambda)$ from Scenario 2, we further examine the impact of diffuse downwelling attenuation coefficient $K_d(\lambda)$ in estimation of backscattering light.
i.e. $I_\lambda = I_o E(0, \lambda) e^{-(K_d(\lambda)d+K_d(\lambda)z)} + V_\lambda^\infty (1 - e^{-K_d(\lambda)z})$
- Scenario 4 (As per the proposed RSUIGM): By considering the influence of $K_d(\lambda)$ in direct scattering, we observe the white patch behaves similar to Jerlov water types classification [49].
i.e. $I_\lambda = I_o E(0, \lambda) e^{-(K_d(\lambda)d+\beta(\lambda)z)} + V_\lambda^\infty (1 - e^{-\beta(\lambda)z})$

We conduct experiments for aforementioned scenarios by considering $z = 1m$ and $d = 1$ to $20m$ and the same range can be further extended as needed. The effect of proposed model as per Equation 19 is shown through white patch behaviour in Fig 6 (a), (b), (c) and (d) corresponding to scenario 1, 2, 3 and 4. The white patch behaviour depicted in Fig 6 and Fig 7 shows irradiance attenuation with depth d is directly proportional to formation of tint in underwater scenes. The white patch behaviour as illustrated in Fig 6 (d) closely replicates the characteristics of Jerlov water types [49]. Unlike Jerlov, who conducted in-situ measurements for characterizing the water types, we are able to simulate the similar behaviour by accurately modeling the degradation parameters. We observe the attenuation coefficients $K_d(\lambda)$ and $\beta(\lambda)$ play a significant role in degradation of underwater scenes. This degradation majorly contributes in loss of color, contrast and other essential features. We observe, $K_d(\lambda)$ and $\beta(\lambda)$ are two different phenomenon, however when considered together, they collectively influence the transmission of light through water, impacting the clarity and appearance of underwater images. Hence, by considering d , z and $K_d(\lambda)$ in estimation of direct scattering and $\beta(\lambda)$ in estimation of backscattering we are able to simulate realistic synthetic underwater scenes.

4 RESULTS AND DISCUSSIONS

In this section, we discuss the results of synthetic data generation considering proposed RSUIGM and show its effect on restoration of underwater images. We generate realistic synthetic underwater taking into account Jerlov water types [37]. Jerlov water types describe the optical properties of water based on factors such as turbidity, mineral content, and depth. By considering these water types in our synthetic data generation process, we aim to simulate a more accurate and diverse representation of underwater environments. We compare RSUIGM dataset with SOTA synthetic data generation techniques and, validate the proposed RSUIGM considering restoration

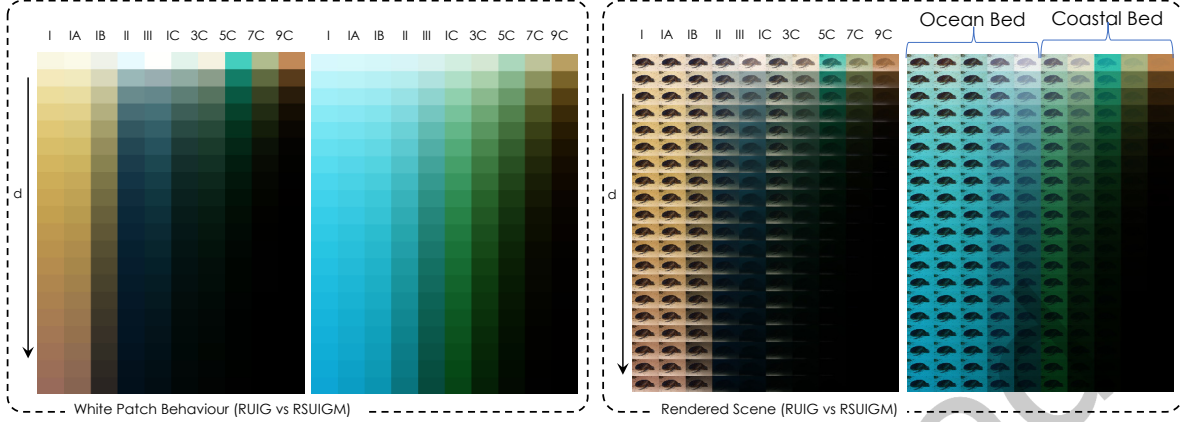


Fig. 7. Comparison of white patch behaviour with SOTA image formation models. The left side shows the behaviour of the white patch generated with RUIG [13] in comparison with proposed RSUIGM, while the right side shows the scene generated with RUIG [13] in comparison with proposed RSUIGM. We infer, the white patch generated using proposed RSUIGM appears visually similar to Jerlov classification [49].

as a framework. Further, we compare the results of restoration with SOTA techniques both qualitatively and quantitatively.

Dataset Description: We use SUID [28] and RUIG [13] for realistic synthetic data generation. SUID dataset [28] contains 30 ground-truth images and 900 corresponding synthetic underwater images of the same scene. RUIG dataset [13] contains 1,60,000 synthetic underwater images. We use UIEB [39] and HICRD [20] real underwater datasets for testing the restoration framework. UIEB dataset contains 890 raw images with corresponding reference images, and 60 challenging underwater images. HICRD dataset contains 6003 original underwater images with 2000 reference restored images.

Experimental Set-up: We generate the realistic synthetic data using Nvidia DGX Tesla V100. We develop the proposed algorithm on Python (v3.8) and PyTorch framework. We generate a total of 6000 images including ocean and coastal beds [37] for varying depths across d and z encompassing the entire distribution of Jerlov classification of water types as shown in Fig 5 and Fig 8.

Table 1. Frechet Inception Distance(FID) shows the quality of generated underwater images. Lower FID score indicates, the distribution of the generated synthetic underwater images is closer to the distribution of real underwater images. Lower FID score implies, the synthetic underwater images are more realistic and capture the statistical properties of real underwater images. Here " \downarrow " indicates lower is better.

Dataset 1	FID Score \downarrow	Dataset 2	FID Score \downarrow
UIEBD vs SUID	280.05	HICRD vs SUID	260.48
UIEBD vs RUIG	240.00	HICRD vs RUIG	290.92
UIEBD vs RSUIGM(Ours)	234.33	HICRD vs RSUIGM(Ours)	249.03



Fig. 8. Generation of synthetic underwater images considering proposed RSUIGM qualitatively. 1st row shows ground-truth images taken from SUID dataset [28], 2nd to 6th and 7th to 11th rows show synthetic underwater images generated using proposed RSUIGM (RSUIGM Dataset) as per ocean and coastal bed [53] respectively.

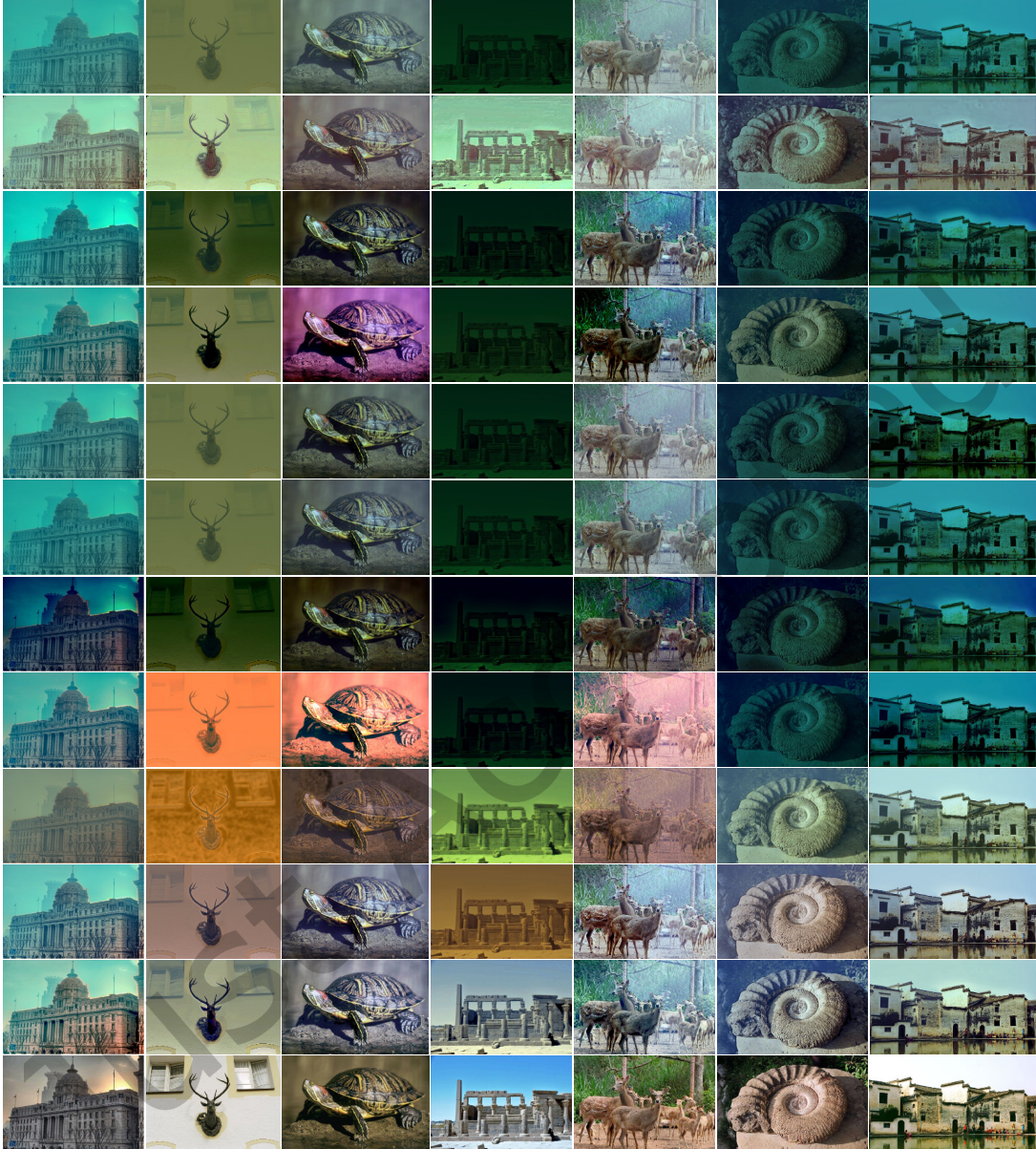


Fig. 9. Restoration of synthetic underwater images in comparison with state-of-the-art methods. 1st row shows input images taken from SUID dataset [28], 2nd to 8th row depicts restoration results of [5, 7, 15, 21, 22, 45, 50] non learning-based techniques, 9th and 10th row shows restoration results of [2, 48] learning-based techniques, 11th row shows the results of restoration with our proposed method DepthCue [9], and 12th row shows the corresponding ground-truth images.



Fig. 10. Restoration results on HICRD [20] dataset. 1st row shows input images, 2nd row shows results from AquaGAN method [10], 3rd row shows results from WaveNet method [48], last row shows results of the DepthCue. We infer recovery of color and contrast is consistent throughout the scene.

4.1 Generation of synthetic underwater images using proposed RSUIGM

In this section, we demonstrate the samples of realistic synthetic underwater images generated using proposed RSUIGM. Fig 8 provides visual representations of samples generated from the learnt distribution of parameters. 1st column shows the ground-truth images, 2nd to 6th columns show the synthesized underwater images as per ocean bed [53], 7th to 11th columns show the synthesized underwater images as per coastal bed [53]. The proposed RSUIGM considers ground-truth images from SUID dataset [28] as true scene radiance for generation of synthetic data. We consider Equation 19 for generation of realistic underwater images. This equation serves as a key element, for guiding the synthesis of realistic underwater scenes.

Unlike [13] and [28], we observe the generated dataset covers larger distribution of water types mimicking the true nature of real underwater images. As shown in Table 1, we use Frechet Inception Distance (FID) [59] as quantitative metric to validate the distribution of synthetically generated underwater images against real underwater images. FID score compares the distribution of synthetically generated images with the distribution of a set of real underwater images. Lower the FID score indicates generated images are closer to real underwater images. We compare the distribution of RSUIGM generated underwater images against two benchmark real underwater datasets namely UIEB [39] and HICR [20] as shown in Table 1.

We observe that RSUIGM simulates realistic appearance of haze, blur, tint, and color attenuation similar to the degraded underwater images. We further validate the proposed RSUIGM dataset, through restoration on real and synthetic underwater images using appropriate quantitative metrics. We claim, the generated RSUIGM dataset provides better restoration performance compared to the other benchmark datasets due to its more realistic underwater image formation process and diverse scene content.

4.1.1 Comparison of RSUIGM dataset with SOTA techniques. We compare the results of RSUIGM dataset with other benchmark synthetic datasets qualitatively as shown in Fig 5. Unlike [13] and [28], we cover a larger distribution of data similar to Jerlov classification [53]. We observe that the generated synthetic underwater

images with the proposed RSUIGM introduces realistic tint and models true color attenuation imitating the distribution of real underwater images. We validate the effectiveness of RSUIGM dataset through white patch behaviour and show the difference in color attenuation of proposed RSUIGM against the authors in [13]. We observe, the white patch and the corresponding scene generated with proposed RSUIGM appears visually similar to Jerlov classification [49] and is shown in Fig 7. The variation of colors in white patch shows the need to consider irradiance attenuation along d in modeling direct light transmission.

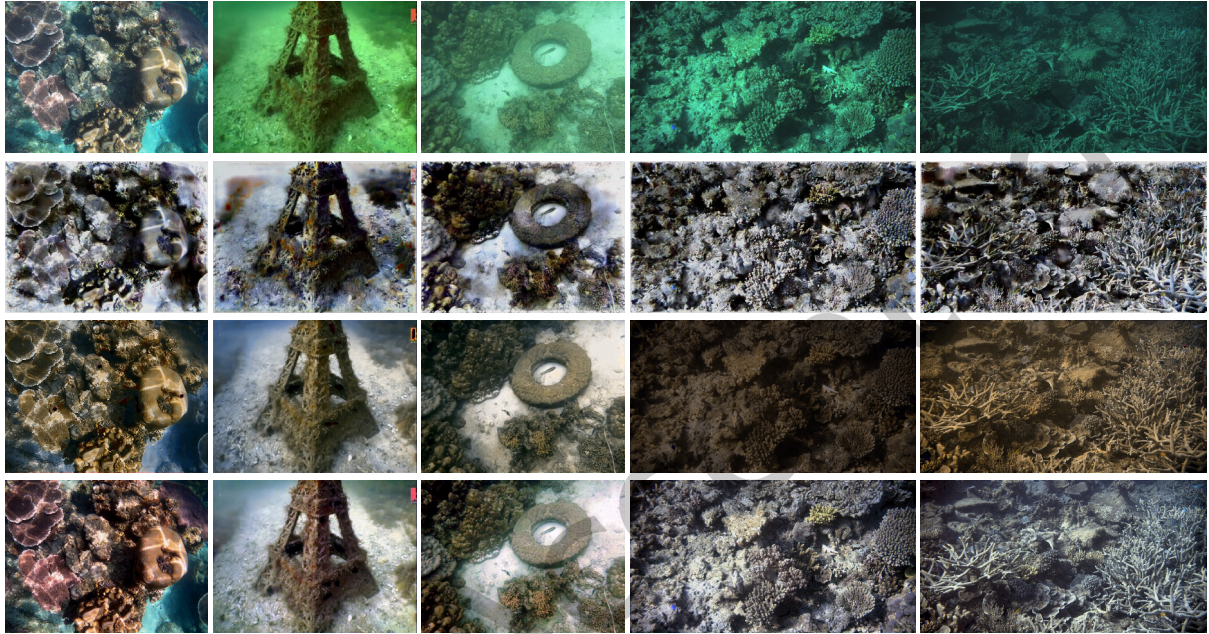


Fig. 11. Restoration with DepthCue considering RUIG [13], SUID [28] and RSUIGM dataset. 1st row shows input images, 2nd row presents the performance of the DepthCue algorithm trained on RUIG [13], 3rd row shows the performance of the DepthCue algorithm trained on SUID [28], last row shows the performance of DepthCue trained with proposed RSUIGM. The results demonstrate the effectiveness of using our proposed model RSUIGM for generating training data, as the restored images show significant improvements in terms of image quality and visual details compared to other SOTA synthetic generation techniques.

4.2 Restoration Framework

We use a learning-based framework DepthCue [9] for restoration of degraded underwater images. DepthCue is a variant of encoder-decoder architecture, and introduces depth as a clue at different scales during restoration. The details of the architecture and the experimental set up is discussed in [9]. We train DepthCue architecture [9] with RSUIGM dataset considering a weighted combinational loss function as discussed by authors [10, 13, 24], and test the performance of the model using real underwater images.

We extend the study, and validate the generalizability of DepthCue restoration framework, by training the architecture with other state-of-the-art synthetic underwater images such as RUIG [13] and SUID [28]. We compare the quality of restoration across the synthetic benchmark datasets by testing the DepthCue model on real underwater images. We demonstrate the results of restoration in Fig 11 and observe consistent improvement in restoration. The improved restoration is a result of training DepthCue architecture with RSUIGM dataset.



Fig. 13. Restoration results on UIEB [39] dataset. 1st row shows input images, 2nd row shows results from AquaGAN method [10], 3rd row shows results from WaveNet method [48], last row shows results of the DepthCue [9]. We infer recovery of color and contrast is consistent throughout the scene.

UFO-120 [31], EUVP [32], HICR [20] and UIEB [39] in comparison with SOTA techniques visually in Fig 10, 12, 13, and 14 respectively. The corresponding quantitative scores are presented in Table 2.

Unlike SOTA techniques, we observe reduction of tint, recovery of color and contrast is consistent throughout the scene as shown in Fig 14, 12, 10 and 13. We observe, the RSUIGM dataset improves the performance of the DepthCue method on both synthetic and real-world underwater images compared to SOTA methods. The results, show the effectiveness and usefulness of the RSUIGM dataset for underwater image restoration tasks. The proposed RSUIGM facilitates generation of larger datasets, creating a paradigm shift in the underwater domain. RSUIGM addresses the limitations of existing underwater image datasets, which are often small in size and limited to the variability of underwater scenes. The RSUIGM dataset overcomes these limitations and provides a diverse collection of underwater images with varying degrees of degradations. However, the images rendered in extreme low light conditions like Jerlov class 3C, 5C, 7C, and 9C with increase in d , requires additional supervision in terms of enhancement [8, 17] and restoration for improving the visibility of scene.

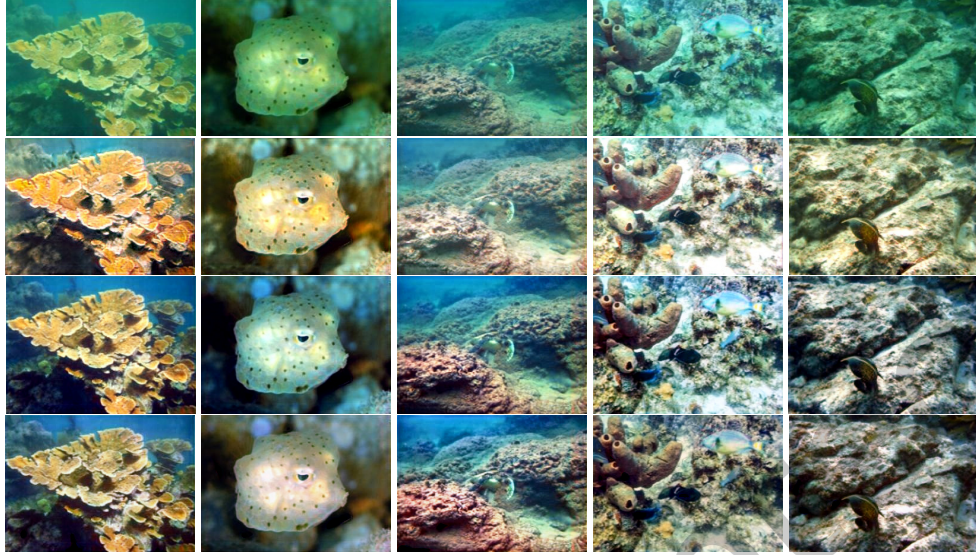


Fig. 14. Restoration results on UFO-120 dataset. 1st row shows input images from UFO-120 dataset [31], 2nd row shows restoration results of [10], 3rd row shows restoration results of [48], 4th row shows restoration results of our methodology [9].

5 CONCLUSIONS

In this paper, we have proposed a model to synthesize realistic underwater images considering both downwelling depth and line of sight (LOS) distance as cue. We have proposed a novel image formation model called the Realistic Synthetic Underwater Image Generation Model (RSUIGM) to incorporate the effect of downwelling depth for generating synthetic underwater images. Unlike existing models that rely on radiative transfer models and in-situ measurements, we have derived the dependencies of downwelling irradiance in direct light estimation to accurately capture the complex light interactions in the ocean. We have demonstrated the effectiveness of our model by generating a large RSUIGM dataset by using it in deep learning-based restoration methods. The quality of synthetic underwater images has been validated using restoration as a framework and compared with state-of-the-art methods on benchmark real underwater image datasets. Our proposed RSUIGM outperforms existing models and achieves improved results, showing its potential for enhancing the accuracy of underwater computer vision applications.

REFERENCES

- [1] Derya Akkaynak and Tali Treibitz. 2019. Sea-Thru: A Method for Removing Water From Underwater Images. In *Proceedings of the IEEE/CVF Conference on Computer Vision and Pattern Recognition (CVPR)*.
- [2] Saeed Anwar, Chongyi Li, and Fatih Porikli. 2018. Deep Underwater Image Enhancement. <https://doi.org/10.48550/ARXIV.1807.03528>
- [3] Yael Bekerman, Shai Avidan, and Tali Treibitz. 2020. Unveiling optical properties in underwater images. In *2020 IEEE International Conference on Computational Photography (ICCP)*. IEEE, 1–12.
- [4] B. Cai, X. Xu, K. Jia, C. Qing, and D. Tao. 2016. DehazeNet: An End-to-End System for Single Image Haze Removal. *IEEE Transactions on Image Processing* 25, 11 (2016), 5187–5198.
- [5] Nicholas Carlevaris-Bianco, Anush Mohan, and Ryan M. Eustice. 2010. Initial results in underwater single image dehazing. In *OCEANS 2010 MTS/IEEE SEATTLE*. 1–8. <https://doi.org/10.1109/OCEANS.2010.5664428>
- [6] Subrahmanyam Chandrasekhar. 2013. *Radiative transfer*. Courier Corporation.

- [7] Liu Chao and Meng Wang. 2010. Removal of water scattering. In *2010 2nd International Conference on Computer Engineering and Technology*, Vol. 2. V2–35–V2–39. <https://doi.org/10.1109/ICCET.2010.5485339>
- [8] Chaitra Desai, Nikhil Akalwadi, Amogh Joshi, Sampada Malagi, Chinmayee Mandi, Ramesh Ashok Tabib, Ujwala Patil, and Uma Mudenagudi. 2023. LightNet: Generative Model for Enhancement of Low-Light Images. In *Proceedings of the IEEE/CVF International Conference on Computer Vision*. 2231–2240.
- [9] Chaitra Desai, Sujay Benur, Ramesh Ashok Tabib, Ujwala Patil, and Uma Mudenagudi. 2023. DepthCue: Restoration of Underwater Images Using Monocular Depth as a Clue. In *Proceedings of the IEEE/CVF Winter Conference on Applications of Computer Vision (WACV) Workshops*. 196–205.
- [10] Chaitra Desai, Badduri Sai Sudheer Reddy, Ramesh Ashok Tabib, Ujwala Patil, and Uma Mudenagudi. 2022. AquaGAN: Restoration of Underwater Images. In *2022 IEEE/CVF Conference on Computer Vision and Pattern Recognition Workshops (CVPRW)*. 295–303. <https://doi.org/10.1109/CVPRW56347.2022.00044>
- [11] Chaitra Desai, Ramesh Ashok Tabib, Anisha Patil, Samanvitha Karanth, Adarsh Jamadandi, Ujwala Patil, and Uma Mudenagudi. 2019. Framework for Underwater Dataset Generation and Classification Towards Modeling Restoration. <https://api.semanticscholar.org/CorpusID:208542448>
- [12] Chaitra Desai, Ramesh Ashok Tabib, Sai Sudheer Reddy, Ujwala Patil, and Uma Mudenagudi. 2021. Rendering of Synthetic Underwater Images Towards Restoration. In *SIGGRAPH Asia 2021 Posters* (Tokyo, Japan) (SA ’21 Posters). Association for Computing Machinery, New York, NY, USA, Article 37, 2 pages. <https://doi.org/10.1145/3476124.3488637>
- [13] Chaitra Desai, Ramesh Ashok Tabib, Sai Sudheer Reddy, Ujwala Patil, and Uma Mudenagudi. 2021. RUIG: Realistic Underwater Image Generation Towards Restoration. In *Proceedings of the IEEE/CVF Conference on Computer Vision and Pattern Recognition (CVPR) Workshops*. 2181–2189.
- [14] Paul Drews, Erickson Nascimento, Filipe Moraes, Silvia Botelho, and Mario Campos. 2013. Transmission estimation in underwater single images. In *Proceedings of the IEEE international conference on computer vision workshops*. 825–830.
- [15] P. Drews Jr, E. do Nascimento, F. Moraes, S. Botelho, and M. Campos. 2013. Transmission Estimation in Underwater Single Images. In *2013 IEEE International Conference on Computer Vision Workshops*. 825–830. <https://doi.org/10.1109/ICCVW.2013.113>
- [16] P. Drews Jr, E. do Nascimento, F. Moraes, S. Botelho, and M. Campos. 2013. Transmission Estimation in Underwater Single Images. In *2013 IEEE International Conference on Computer Vision Workshops*. 825–830. <https://doi.org/10.1109/ICCVW.2013.113>
- [17] Egor Ershov, Alex Savchik, Denis Shepelev, Nikola Banić, Michael S Brown, Radu Timofte, Karlo Kočević, Michael Freeman, Vasily Tesalin, Dmitry Bocharov, et al. 2022. NTIRE 2022 challenge on night photography rendering. In *Proceedings of the IEEE/CVF Conference on Computer Vision and Pattern Recognition*. 1287–1300.
- [18] Raanan Fattal. 2008. Single Image Dehazing. *ACM Trans. Graph.* 27, 3 (Aug. 2008), 1–9. <https://doi.org/10.1145/1360612.1360671>
- [19] Adrian Galdran, David Pardo, Artzai Picón, and Aitor Alvarez-Gila. 2015. Automatic Red-Channel underwater image restoration. *Journal of Visual Communication and Image Representation* 26 (2015), 132–145. <https://doi.org/10.1016/j.jvcir.2014.11.006>
- [20] Junlin Han, Mehrdad Shoeiby, Tim Malthus, Elizabeth Botha, Janet Anstee, Saeed Anwar, Ran Wei, Ali Armin, Hongdong Li, and Lars Petersson. 2021. Underwater Image Restoration via Contrastive Learning and a Real-world Dataset.
- [21] Junlin Han, Mehrdad Shoeiby, Tim Malthus, Elizabeth Botha, Janet Anstee, Saeed Anwar, Ran Wei, Lars Petersson, and Mohammad Ali Armin. 2021. Single Underwater Image Restoration by Contrastive Learning. <https://doi.org/10.48550/ARXIV.2103.09697>
- [22] Kaiming He, Jian Sun, and Xiaou Tang. 2010. Single image haze removal using dark channel prior. *IEEE transactions on pattern analysis and machine intelligence* 33, 12 (2010), 2341–2353.
- [23] K. He, J. Sun, and X. Tang. 2011. Single Image Haze Removal Using Dark Channel Prior. *IEEE Transactions on Pattern Analysis and Machine Intelligence* 33, 12 (2011), 2341–2353.
- [24] Dikshit Hegde, Tejas Anvekar, Ramesh Ashok Tabib, and Uma Mudengudi. 2022. DA-AE: Disparity-Alleviation Auto-Encoder Towards Categorization of Heritage Images for Aggrandized 3D Reconstruction.. In *Proceedings of the IEEE/CVF Conference on Computer Vision and Pattern Recognition*. 5093–5100.
- [25] Deepthi Hegde, Chaitra Desai, Ramesh Tabib, Uma Mudenagudi, and Prabin Kumar Bora. [n. d.]. Adaptive Color Correction for Underwater Image Enhancement. ([n. d.].)
- [26] Deepthi Hegde, Chaitra Desai, Ramesh Tabib, Ujwala B. Patil, Uma Mudenagudi, and Prabin Kumar Bora. 2020. Adaptive Cubic Spline Interpolation in CIELAB Color Space for Underwater Image Enhancement. *Procedia Computer Science* 171 (2020), 52–61. <https://doi.org/10.1016/j.procs.2020.04.006> Third International Conference on Computing and Network Communications (CoCoNet’19).
- [27] Deepthi Hegde, Dikshit Hegde, Ramesh Ashok Tabib, and Uma Mudenagudi. 2020. Relocalization of camera in a 3d map on memory restricted devices. In *Computer Vision, Pattern Recognition, Image Processing, and Graphics: 7th National Conference, NCVPRIPG 2019, Hubballi, India, December 22–24, 2019, Revised Selected Papers 7*. Springer, 548–557.
- [28] Guojia Hou, Xin Zhao, Zhenkuan Pan, Huan Yang, Lu Tan, and Jingming Li. 2020. Benchmarking underwater image enhancement and restoration, and beyond. *IEEE Access* 8 (2020), 122078–122091.
- [29] Weilin Hou, Deric J. Gray, Alan D. Weidemann, Georges R. Fournier, and J. L. Forand. 2007. Automated underwater image restoration and retrieval of related optical properties. In *2007 IEEE International Geoscience and Remote Sensing Symposium*. 1889–1892. <https://doi.org/10.1109/IGARSS.2007.4387467>

- [56] Craig A Williamson and Richard C Hollins. 2022. Measured IOPs of Jerlov water types. *Applied Optics* 61, 33 (2022), 9951–9961.
- [57] George Wypych. 2020. *Handbook of UV degradation and stabilization*. Elsevier.
- [58] Tian Ye, Sixiang Chen, Yun Liu, Yi Ye, Erkang Chen, and Yuche Li. 2022. Underwater light field retention: Neural rendering for underwater imaging. In *Proceedings of the IEEE/CVF Conference on Computer Vision and Pattern Recognition*. 488–497.
- [59] Yu Yu, Weibin Zhang, and Yun Deng. 2021. Frechet inception distance (fid) for evaluating gans. *China University of Mining Technology Beijing Graduate School* (2021).
- [60] He Zhang, Vishwanath Sindagi, and Vishal M. Patel. 2020. Joint Transmission Map Estimation and Dehazing Using Deep Networks. *IEEE Transactions on Circuits and Systems for Video Technology* 30, 7 (2020), 1975–1986. <https://doi.org/10.1109/TCSVT.2019.2912145>
- [61] Mohua Zhang and Jianhua Peng. 2018. Underwater Image Restoration Based on A New Underwater Image Formation Model. *IEEE Access* 6 (2018), 58634–58644. <https://doi.org/10.1109/ACCESS.2018.2875344>
- [62] Song Zhang, Shili Zhao, Dong An, Jincun Liu, He Wang, Yu Feng, Daoliang Li, and Ran Zhao. 2022. Visual SLAM for underwater vehicles: A survey. *Computer Science Review* 46 (2022), 100510.